Journal of Organometallic Chemistry, 376 (1989) 297–310
Elsevier Sequoia S.A., Lausanne – Printed in The Netherlands
JOM 20143

Synthesis and structures of two new mixed antimony-iron carbonyl clusters: $[R_4N][SbFe_4(CO)_{16}]$ (R = Me, Et) and $[Et_4N]_2[Sb_2Fe_6(CO)_{20}]$

Shifang Luo and Kenton H. Whitmire *

Department of Chemistry, Rice University, P.O. Box 1892, Houston, TX 77251 (U.S.A.)

(Received April 25th, 1989)

Abstract

$[R_4N][SbFe_4(CO)_{16}]$ ($[R_4N][I]$, R = Me, Et) was prepared by the oxidation of $[R_4N]_3[SbFe_4(CO_{16})]$ with two equivalents of $[Cu(MeCN)_4][BF_4]$. Single crystal X-ray diffraction of $[Me_4N][I]$ shows that it crystallizes in the triclinic centrosymmetric space group $P\bar{1}$ with a 11.840(3) Å, b 12.550(3) Å, c 10.500(2) Å, α 94.41(2)°, β 101.14(2)°, γ 89.20(2)°, V 1526.3(6) Å^3 and $Z = 2$. Full matrix least squares refinement on a basis of 5072 unique reflections led to $R = 0.036$, $R_w = 0.049$. The anion has a highly distorted tetrahedral core in which the four-coordinate antimony atom is surrounded by two isolated $Fe(CO)_4$ units and an $Fe_2(CO)_8$ group. Photolysis of $[Et_4N][I]$ with UV light gave as the only cluster product $[Et_4N]_2[Sb_2Fe_6(CO)_{20}]$ ($[Et_4N]_2[II]$) which can also be prepared by the reaction of $[Et_4N]_2[Fe_4(CO)_{13}]$ with $SbCl_3$. It crystallizes with 0.941(9) molecule of solvent CH_2Cl_2 in orthorhombic accentric space group $P2_12_12_1$ with a 15.962(6) Å, b 25.878(6) Å, c 10.035(2) Å, V 5384(2) Å^3 and $Z = 4$. The anion has a distorted *trans*-Sb_2Fe_4 octahedral core in which each Sb atom is bonded to an external $Fe(CO)_4$ unit. Full matrix least squares refinement on a basis of 4007 unique reflections converged with $R = 0.040$ and $R_w = 0.049$.

Introduction

Recent advances in the chemistry of mixed heavy main group element/transition metal clusters has revealed the important role played by the main group elements [1–3]. Intriguing structures and bonding patterns have been found. Multiple bonding has been proposed as in $[(\mu_3,\eta^2\text{-}E_2)\{W(CO)_5\}_3]$ (E = As, Sb, Bi) which display very short E–E distances [4a–4c]. Electron deficient EM_3 molecules like

0022-328X/89/$03.50

$[CpMn(CO)_2]_3As$ [5], $[\{C_5Me_5(CO)_2Mn\}_2As][BF_4]$ [6], $[Cr(CO)_5]_2[Mn(CO)_5]As$ [7], $[Cr_2(CO)_9][Mn(CO)_5]As$ [7], $[Mn\{\eta^5\text{-}C_5H_4Me)(CO)_2]_3Te$ [8] and $[Et_4N]_2[EFe_3(CO)_{12}]$ (E = Pb, Sn) [9] are also known while hypervalent bonding situations have been observed in $[Cp_2Co][Bi\{Co(CO)_4\}_4]$ [10] and $CpMoFe(CO)_5\{Te_2X\}$ (X = Br, S_2CNEt_2) [11]. The unusual arsenic and phosphorus complexes $Cp_2Mo_2As_5$ [12] and $(C_5Me_5)_2Mo_2P_6$ [13] have been recently reported. The cluster framework of $[Et_4N]_2[Bi_4Fe_4(CO)_{13}]$ [14,15] has relationship to that of the discrete Zintl cluster phases [16]. The main group constituents in these prominent examples strongly influence the chemical and structural patterns observed.

We have pursued study of the interactions of the heavier main group V elements with iron and cobalt carbonyls and a number of new heteroatomic clusters have been synthesized and characterized. Comparisons between bismuth and antimony have been insightful in understanding the roles played by these heavier main group elements [17,18]. In this paper we report the syntheses and structures of two new members of the Sb–Fe carbonyl cluster family: $[R_4N][SbFe_4(CO)_{16}]$ ($[R_4N][I]$, R = Me, Et) and $[Et_4N]_2[Sb_2Fe_6(CO)_{20}]$ ($[Et_4N][II]$).

Experimental

All experiments were performed under an atmosphere of dry N_2 using standard Schlenk techniques. Commercial reagents were used without purification except $SbCl_3$ which was sublimed before use. $[R_4N]_3[SbFe_4(CO)_{16}]$ [18], $[Cu(MeCN)_4][BF_4]$ [19] and $[Et_4N]_2[Fe_4(CO)_{13}]$ [20] were prepared according to published methods. Organic solvents were distilled from standard drying agents and purged with N_2 for about 20 min before use. Infrared spectra were taken on a PE 1600 FTIR spectrophotometer and the elemental analyses were obtained from Galbraith Laboratories, Inc.

Preparation of $[Et_4N][SbFe_4(CO)_{16}]$. $[Et_4N]_3[SbFe_4(CO)_{16}]$ (1.373 g, 1.160 mmol) and $[Cu(MeCN)_4][BF_4]$ (0.730 g, 2.320 mmol) were weighed into a 100 ml Schlenk flask. The mixture was dissolved in 30 ml MeCN and the red solution turned dark brown within a few minutes while copper powder precipitated from the solution. Stirring was continued overnight. The solution was filtered through a medium porosity glass filter frit and the MeCN was removed from the filtrate under vacuum. The solid residue was dissolved in 30 ml CH_2Cl_2 and filtered. Black needle-like crystals grew by slow diffusion when two volumes of hexanes were layered on top of the filtrate. Yield: 0.84 g, 79% (based on Sb). Similar results were obtained for the $[Me_4N]^+$ salt of $[I]^{1-}$. $[R_4N][SbFe_4(CO)_{16}]$ is soluble in CH_2Cl_2, MeOH, acetone, MeCN and THF. IR (in CH_2Cl_2, cm^{-1}): 2086(w), 2042(s), 2020(vs), 1922(s). A single crystal of $[Me_4N][SbFe_4(CO)_{16}]$ suitable for X-ray diffraction was grown from a concentrated cooled CH_2Cl_2 solution.

Reduction of $[Et_4N][SbFe_4(CO)_{16}]$ with Na/Hg. $[Et_4N][SbFe_4(CO)_{16}]$ (0.924 g, 1.000 mmol) were placed in a Schlenk flask and dissolved in 30 ml MeCN. The solution was added to sodium amalgam (0.08 g Na in 40.0 g Hg) solution. The dark brown solution turned red in about 1 min, was stirred for 30 min and then filtered through celite. The filtrate was concentrated and treated with excess $[Et_4N]Br$ dissolved in methanol. The red precipitate thus obtained was collected by filtration and dried under vacuum. Yield 0.77 g, 65% (based on Sb).

Preparation of $[Et_4N]_2[Sb_2Fe_6(CO)_{20}]$. (a) Reaction of $[Et_4N]_2[Fe_4(CO)_{13}]$

with $SbCl_3$: $SbCl_3$ (0.200 g, 0.877 mmol) and $[Et_4N]_2[Fe_4(CO)_{13}]$ (0.892 g, 1.052 mmol) were placed in a 100 ml Schlenk flask. The mixture was dissolved in 30 ml CH_2Cl_2 and heated to reflux overnight. The next day the solution was filtered and the solvent was removed under vacuum. The solid residue was extracted with 20 ml portions of Et_2O until the extract was colorless. The Et_2O extract was proven to be $[Et_4N][SbFe_4(CO)_{14}]$ according to its IR spectrum (yield: 15%, based on Sb). The solid residue was dissolved in 30 ml CH_2Cl_2 and precipitated with 60 ml Et_2O. The brown solid thus obtained was collected by filtration and dried under vacuum. Yield: 0.49 g, 80% (based on Sb).

(b) Photolysis of $[Et_4N][SbFe_4(CO)_{16}]$. $[Et_4N][SbFe_4(CO)_{16}]$ (0.509 g, 0.549 mmol) was placed in a 100 ml Schlenk flask and dissolved in 30 ml MeOH. The solution was irradiated by a 400 W Ace Hannovia Mercury Arc Lamp until infrared measurements showed that the band at 2086 cm^{-1} from the parent had totally disappeared. This solution was filtered and the MeOH removed under vacuum. The solid residue was dissolved in 30 ml CH_2Cl_2, filtered, concentrated and cooled in a freezer ($-20\,°C$). Crystals of $[Et_4N]_2[Sb_2Fe_6(CO)_{20}]$ grew from the solution. Yield: 0.22 g, 58% (based on Sb). $[Et_4N]_2[Sb_2Fe_6(CO)_{20}]$ is soluble in CH_2Cl_2, MeOH, acetone, MeCN and THF. IR (in CH_2Cl_2, cm^{-1}) 2019(s), 1988(vs), 1961(m), 1929(s). Anal. (assuming no loss of lattice solvent). Found: Sb, 16.25; Fe, 22.74. $C_{36}H_{40}Fe_6N_2O_{20}Sb_2$ calcd.: Sb, 16.40; Fe, 22.58%. A crystal suitable for single crystal X-ray diffraction was grown from a concentrated, cooled CH_2Cl_2 solution.

X-ray single crystal structure determination

Crystallographic data collection parameters for $[Me_4N][I]$ and $[Et_4N]_2[II]$ are presented in Table 1. In both cases the single crystals were mounted on a glass fiber and fixed by Epoxy glue. Crystal data for $[Me_4N][I]$ indicated a triclinic space group and the more common centrosymmetric setting $P\bar{1}$ (No. 2) was chosen and subsequently shown to be correct by successful data solution and refinement. The heavy atoms were located by MITHRIL [21]. All non-hydrogen atoms were located in difference maps from following refinements using the TEXSAN(2.0) structure solution package (Molecular Structure Corporation). Disorder in the carbon positions of the $[Me_4N]^+$ cations was resolved into two sets and these were refined as rigid groups. For the two sets the relative populations refined to a 60(2)/40(2) ratio. All non-hydrogen atoms except those of the $[Me_4N]^+$ cations were refined anisotropically

For $[Et_4N]_2[II]$, crystal data indicated an acentric, orthorhombic space group $P2_12_12_1$ (No. 19). The α carbon atoms of the $[Et_4N]^+$ cations are disordered but were resolved into two different sets. These two sets were refined to give relative populations in 64(2)/36(2) and 51(2)/49(2) ratios for the first and second cations, respectively. In the latter stages of refinement, solvent CH_2Cl_2 was observed in the difference maps and its population was refined since some crystal decay due to solvent loss seemed to occur. The population at convergence was 0.941(9). The hydrogen atoms on the solvent molecules were included in calculated positions but not refined. All non-hydrogen atoms except the carbon atoms of the cations were refined anisotropically while the cation carbons were refined isotropically. Structure solution and refinement methodology followed that for $[Me_4N][I]$. Both enantiomorphs were checked since the space group is acentric. The chosen form gave residuals 0.2% less than those of the other enantiomorph.

Results and discussion

Synthesis and reduction of [R_4N][I]. The oxidation of the trianion $[SbFe_4(CO)_{16}]^{3-}$ by two equivalents of $[Cu(MeCN)_4][BF_4]$ gives the monoanion $[I]^{1-}$, in which the loss of two electrons is compensated for by the formation of an Fe–Fe bond. Along with the oxidation process, the coordination sphere around the Sb atom changes dramatically from a regular to a highly distorted tetrahedron. The process is chemically reversible; reduction of the monoanion $[I]^{1-}$ with sodium amalgam gives back the trianion (see Scheme 1). The monoanion is isoelectronic with $[PbFe_4(CO)_{16}]^{2-}$ [22] and $[EFe_3Cr(CO)_{17})]^{1-}$ (E = Sb, Bi) [23] which also contain central main group atoms coordinated by two isolated ML_n moieties and an $Fe_2(CO)_8$ group. Attempts at further oxidation to produce spiro-$[Sb\{Fe_2(CO)_8\}_2]^+$ with two Fe–Fe bonds, isoelectronic and isostructural with neutral $E\{Fe_2(CO)_8\}_2$

Table 1

Crystallographic parameters for $[Me_4N][I]$ and $[Et_4N]_2[II]\cdot 0.94\ CH_2Cl_2$

	$[Me_4N][I]$	$[Et_4N]_2[II]\cdot 0.94\ CH_2Cl_2$
Empirical formula	$SbFe_4C_{20}H_{12}O_{16}N$	$Sb_2Fe_6C_{37}H_{42}O_{20}N_2Cl_2$
Formula weight	867.45	1484.22
Crystal system	triclinic	orthorhombic
Space group	$P\bar{1}$ (No. 2)	$P2_12_12_1$ (No. 19)
a, Å	11.840(3)	15.962(6)
b, Å	12.550(3)	25.878(6)
c, Å	10.500(2)	13.035(2)
α, deg	94.41(2)	90
β, deg	101.14(2)	90
γ, deg	89.20(2)	90
V, Å^3	1526.3(6)	5384(2)
Z	2	4
ρ_{calc}, g cm^{-3}	1.89	1.82
Temperature (K)	296	296
Color	black	black
Size (mm)	$0.30\times0.30\times0.50$	$0.30\times0.40\times0.50$
μ, cm^{-1} (Mo-K_α)	28.04	27.22
T_{max}/T_{min}	1.0000/0.8152	1.0000/0.7310
Diffractometer	Rigaku AFC5S	
Radiation (Å)	Mo-K_α (λ 0.71069 Å)	
Monochromator	Graphite	
2θ limit	4.0–55.0	4.0–55.0
Indep. rflns	7014	5993
Unique rflns [$I > 3\sigma(I)$]	5072	4007
Standard rflns	3 stds/150 rflns	
Scan method	$\omega/2\theta$	
Decay	none observed	
No variables	353	574
R, %	3.6	4.0
R_w, %	4.9	4.9
GOF	1.35	1.21
$\Delta(r)$, e/Å^3	0.79	0.55

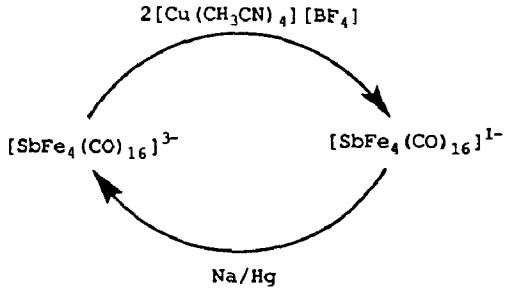

Scheme 1

(E = Ge, Sn, Pb) [24–26] were not fruitful. Very few spiro-cationic clusters of this type are known with the exception of $[As\{Co(CO)Cp\}_4]^+$ [27].

Synthesis of $[Et_4N]_2$[II]. Two distinct reactions have been observed leading to the formation of $[Et_4N]_2$[II]. Photolysis of $[Et_4N][SbFe_4(CO)_{16}]$ with UV light for ~ 48 h gives a solution whose infrared spectrum shows as the only cluster product $[Et_4N]_2$[II]. The previously reported $[Et_4N][SbFe_4(CO)_{14}]$ [28] was observed as a by-product if the reaction was stopped earlier. It would appear that the production of $[Et_4N]_2$[II] may be induced by the cleavage of an $Sb–Fe(CO)_4$ bond with the resultant dimerization of the hypothetical "$SbFe_3$" fragments (see Scheme 2). Such dimerization is observed in the conversions of other antimony-containing iron carbonyl species [23].

The second synthetic method is the reaction of $SbCl_3$ with $[Et_4N]_2[Fe_4(CO)_{13}]$. The reaction was first done to produce $[Et_4N][SbFe_4(CO)_{14}]$ [28] in analogy to the reaction of PCl_3 which was known to give the isostructural $[Et_4N][PFe_4(CO)_{14}]$ [29]. Unlike the reaction of PCl_3, the major product of the reaction with $SbCl_3$ is $[Et_4N]_2$[II] (80% based on Sb) along with a small quantity of $[Et_4N][SbFe_4(CO)_{14}]$ (15% based on Sb).

Crystal structure of $[Me_4N]$[I]. The crystal structure of $[Me_4N]$[I] contains ordered $[SbFe_4(CO)_{16}]^{1-}$ anions and disordered $[Me_4N]^+$ cations in the ratio of 1/1. Selected atomic positional and thermal parameters are given in Table 2 with

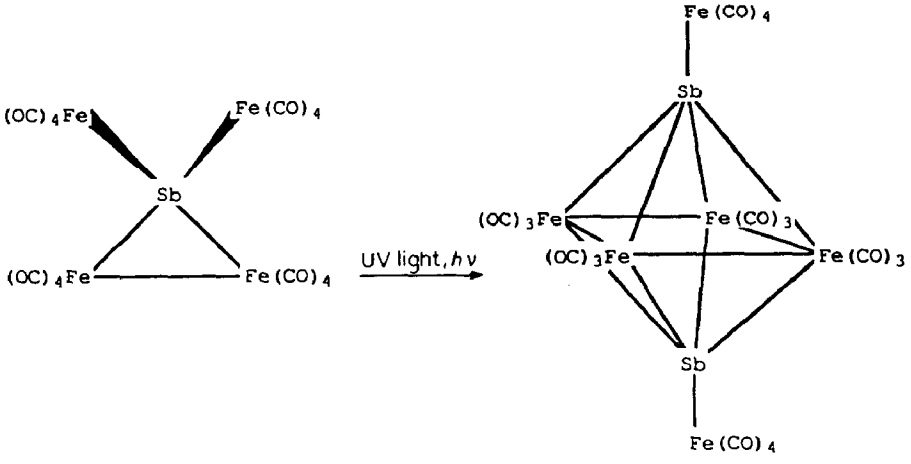

Scheme 2

Table 2

Selected positional parameters and B_{eq} for $[Me_4N][I]$

Atom	x	y	z	B_{eq}
Sb1	0.27991(2)	0.25589(2)	0.30236(3)	3.29(1)
Fe1	0.23541(5)	0.38063(5)	0.49973(6)	3.55(2)
Fe2	0.15859(5)	0.17528(5)	0.45863(7)	3.70(3)
Fe3	0.17426(6)	0.28507(6)	0.06963(7)	4.20(3)
Fe4	0.48601(6)	0.18598(6)	0.31238(8)	4.71(3)
O11	0.4865(3)	0.3861(4)	0.5944(5)	7.2(2)
O12	−0.0178(3)	0.3784(3)	0.4410(5)	6.6(2)
O13	0.2314(5)	0.5755(4)	0.3652(5)	8.1(3)
O14	0.2140(4)	0.4838(3)	0.7547(4)	6.6(2)
O21	−0.0382(3)	0.1543(4)	0.2384(5)	7.4(2)
O22	0.3172(4)	0.2036(3)	0.7118(4)	5.9(2)
O23	0.2542(4)	−0.0332(3)	0.3928(5)	6.8(2)
O24	0.0000(5)	0.1078(4)	0.6198(5)	9.2(3)
O31	0.0182(5)	0.4387(5)	0.1659(5)	9.3(3)
O32	0.3858(4)	0.3614(5)	0.0032(5)	8.8(3)
O33	0.1319(5)	0.0535(4)	0.0416(6)	9.2(3)
O34	0.0531(4)	0.3069(4)	−0.1967(4)	8.0(2)
O41	0.4047(5)	0.0509(5)	0.0736(7)	11.5(4)
O42	0.5576(5)	0.4015(4)	0.2827(6)	9.9(3)
O43	0.4898(4)	0.1146(4)	0.5718(4)	6.8(2)
O44	0.7159(5)	0.0993(7)	0.3179(7)	13.9(5)
C11	0.3903(5)	0.3788(4)	0.5537(5)	4.6(2)
C12	0.0787(5)	0.3633(4)	0.4571(5)	5.1(2)
C13	0.2324(5)	0.4980(5)	0.4131(6)	5.1(2)
C14	0.2191(4)	0.4419(4)	0.6571(5)	4.4(2)
C21	0.0408(5)	0.1656(4)	0.3206(6)	5.1(2)
C22	0.2624(4)	0.2062(4)	0.6089(5)	4.5(2)
C23	0.2196(4)	0.0478(4)	0.4191(5)	4.7(2)
C24	0.0607(5)	0.1375(5)	0.5603(6)	5.5(2)
C31	0.0795(5)	0.3779(5)	0.1313(5)	5.6(3)
C32	0.3045(5)	0.3310(5)	0.0352(6)	5.6(3)
C33	0.1491(5)	0.1452(5)	0.0535(6)	6.0(3)
C34	0.1019(5)	0.2984(5)	−0.0919(6)	5.6(3)
C41	0.4327(6)	0.1038(5)	0.1675(8)	6.7(3)
C42	0.5270(5)	0.3189(5)	0.2960(7)	6.0(3)
C43	0.4853(4)	0.1423(4)	0.4703(6)	5.2(2)
C44	0.6242(6)	0.1311(7)	0.3156(7)	8.2(4)

selected bond distances and angles provided in Table 4. The anion has a highly distorted tetrahedral $SbFe_4$ core in which the central Sb atom is bound to four Fe atoms, two of which belong to two isolated $Fe(CO)_4$ units with an average Sb-Fe bond distance of 2.570(3) Å, the other two belong to an $Fe_2(CO)_8$ unit with an average Sb–Fe bond distance of 2.637(8) Å. Symmetrically bridging CO's which are observed in the isoelectronic species $[PbFe_4(CO)_{16}]^{2-}$ and $[EFe_3Cr(CO)_{17}]^{1-}$ (E = Bi, Sb) anions are absent here. However, the distances between Fe(1)–C(22) (2.536 Å) and Fe(2)–C(12) (2.530 Å) and the bond angles of Fe(1)–C(12)–O(12) (163.1(5)°) and Fe(2)–C(22)–O(22) (163.5(5)°) indicate some semi-bridging character [30] in the bonding of these two CO's. The longer bond distances of Fe(1)–C(12) (1.835(6) Å) and Fe(2)–C(22) (1.822(5) Å) also support this. The lower charge in $[I]^{1-}$ as

Table 3

Selected positional parameters and B_{eq} for $[Et_4N]_2[II]\cdot 0.94CH_2Cl_2$

Atom	x	y	z	B_{eq}
Sb1	0.63838(5)	0.12579(3)	0.60390(5)	3.41(3)
Sb2	0.48257(6)	0.04407(3)	0.55839(6)	3.67(3)
Fe1	0.4930(1)	0.10816(6)	0.7042(1)	3.96(7)
Fe2	0.6219(1)	0.03566(6)	0.6736(1)	3.88(8)
Fe3	0.6176(1)	0.05488(6)	0.4603(1)	3.84(7)
Fe4	0.5085(1)	0.14064(6)	0.4980(1)	3.62(7)
Fe5	0.7582(1)	0.18835(7)	0.6345(1)	4.40(8)
Fe6	0.3656(1)	−0.01797(7)	0.5114(2)	5.6(1)
O11	0.3291(7)	0.1535(4)	0.689(1)	7.9(6)
O12	0.5590(8)	0.1802(5)	0.8581(7)	8.1(7)
O13	0.4327(7)	0.0310(5)	0.8483(9)	8.3(7)
O21	0.7917(7)	0.0032(5)	0.633(1)	9.8(8)
O22	0.5621(8)	−0.0682(4)	0.727(1)	8.7(7)
O23	0.6645(8)	0.0629(5)	0.8816(8)	8.7(7)
O31	0.7875(7)	0.0788(5)	0.396(1)	9.3(8)
O32	0.6327(9)	−0.0572(4)	0.453(1)	8.9(7)
O33	0.5476(8)	0.0586(5)	0.2547(9)	9.3(8)
O41	0.3379(6)	0.1352(4)	0.4156(8)	7.2(6)
O42	0.5871(7)	0.1840(4)	0.3164(9)	8.4(7)
O43	0.4814(7)	0.2427(4)	0.5814(8)	7.1(6)
O51	0.9071(7)	0.2492(4)	0.6712(9)	7.6(6)
O52	0.7767(9)	0.2004(5)	0.4135(8)	8.8(7)
O53	0.6450(8)	0.2639(4)	0.730(1)	9.9(8)
O54	0.8350(8)	0.1061(5)	0.755(1)	10.2(8)
O61	0.228(1)	−0.0796(9)	0.442(2)	26(2)
O62	0.2741(8)	0.0236(6)	0.685(1)	11(1)
O63	0.464(1)	−0.1120(5)	0.545(1)	12(1)
O64	0.369(1)	0.0265(5)	0.307(1)	9.9(8)
C11	0.3951(9)	0.1352(5)	0.693(1)	5.1(6)
C12	0.5366(8)	0.1519(5)	0.794(1)	5.0(7)
C13	0.457(1)	0.0615(6)	0.790(1)	5.7(7)
C21	0.725(1)	0.0167(6)	0.648(1)	5.7(7)
C22	0.5789(9)	−0.0279(5)	0.701(1)	5.1(7)
C23	0.6488(8)	0.0525(5)	0.798(1)	5.1(6)
C31	0.7219(8)	0.0723(6)	0.425(1)	5.5(7)
C32	0.625(1)	−0.0123(5)	0.459(1)	5.8(7)
C33	0.5746(8)	0.0568(5)	0.338(1)	5.0(7)
C41	0.4038(9)	0.1330(6)	0.449(1)	5.4(7)
C42	0.5580(8)	0.1662(5)	0.389(1)	4.8(6)
C43	0.4923(8)	0.2014(5)	0.554(1)	5.2(6)
C51	0.849(1)	0.2262(5)	0.655(1)	5.4(7)
C52	0.768(1)	0.1947(5)	0.500(1)	5.9(8)
C53	0.688(1)	0.2331(6)	0.690(1)	5.9(7)
C54	0.8011(9)	0.1384(6)	0.707(1)	6.1(8)
C61	0.282(1)	−0.0575(8)	0.470(2)	11(1)
C62	0.311(1)	0.0072(1)	0.612(2)	9(1)
C63	0.429(1)	−0.0736(7)	0.535(1)	7(1)
C64	0.370(1)	0.0100(6)	0.388(1)	6.8(8)

Table 4. Selected bond distances (Å) and angles (deg) of $[Me_4N][I]$

(a) Distances			
Sb1–Fe1	2.631(1)	C11–O11	1.139(7)
Sb1–Fe2	2.643(1)	C12–O12	1.138(7)
Sb1–Fe3	2.572(1)	C13–O13	1.128(8)
Sb1–Fe4	2.567(1)	C14–O14	1.128(7)
Fe1–Fe2	2.720(1)	C21–O21	1.146(7)
Fe1–C11	1.812(5)	C22–O22	1.151(6)
Fe1–C12	1.835(6)	C23–O23	1.125(7)
Fe1–C13	1.786(6)	C24–O24	1.124(9)
Fe1–C14	1.812(5)	C31–O31	1.133(8)
Fe2–C21	1.805(5)	C32–O32	1.157(9)
Fe2–C22	1.822(5)	C33–O33	1.165(8)
Fe2–C23	1.799(6)	C34–O34	1.151(7)
Fe2–C24	1.811(7)	C41–O41	1.14(1)
Fe3–C31	1.779(6)	C42–O42	1.130(9)
Fe3–C32	1.765(7)	C43–O43	1.151(7)
Fe3–C33	1.774(7)	C44–O44	1.15(1)
Fe3–C34	1.765(6)	Fe4–C41	1.784(7)
Fe4–C42	1.774(7)	Fe4–C43	1.788(7)
Fe4–C44	1.763(8)		
(c) Angles			
Fe1–Sb1–Fe2	62.09(3)	Fe1–Sb1–Fe3	119.91(3)
Fe1–Sb1–Fe4	118.48(3)	Fe2–Sb1–Fe3	117.04(3)
Fe2–Sb1–Fe4	117.07(3)	Fe3–Sb1–Fe4	113.13(3)
Sb1–Fe1–Fe2	59.17(3)	Sb1–Fe1–C11	83.6(2)
Sb1–Fe1–C12	95.4(2)	Sb1–Fe1–C13	92.7(2)
Sb1–Fe1–C14	166.9(2)	C11–Fe1–Fe2	108.4(2)
C11–Fe1–C12	171.2(2)	C11–Fe1–C13	95.6(2)
C11–Fe1–C14	90.2(2)	C12–Fe1–Fe2	62.1(2)
C12–Fe1–C13	93.2(3)	C12–Fe1–C14	88.9(2)
C13–Fe1–Fe2	139.3(2)	C13–Fe1–C14	99.3(2)
C14–Fe1–Fe2	112.6(2)	Sb1–Fe2–Fe1	58.74(3)
Sb1–Fe2–C21	86.6(2)	Sb1–Fe2–C22	96.3(2)
Sb1–Fe2–C23	86.9(2)	Sb1–Fe2–C24	171.1(2)
C21–Fe2–Fe1	109.0(2)	C21–Fe2–C22	169.9(2)
C21–Fe2–C23	94.8(2)	C21–Fe2–C24	89.0(3)
C22–Fe2–Fe1	64.4(2)	C22–Fe2–C23	95.7(2)
C22–Fe2–C24	86.8(3)	C23–Fe2–Fe1	135.5(2)
C23–Fe2–C24	101.1(1)	C24–Fe2–Fe1	115.9(2)
C31–Fe3–Sb1	90.6(2)	C32–Fe3–Sb1	89.0(2)
C33–Fe3–Sb1	85.8(2)	C34–Fe3–Sb1	177.2(2)
C31–Fe3–C32	119.5(3)	C31–Fe3–C33	122.5(3)
C31–Fe3–C34	91.4(3)	C32–Fe3–C33	117.8(3)
C32–Fe3–C34	91.6(3)	C33–Fe3–C34	91.5(3)
Sb1–Fe4–C41	87.7(2)	Sb1–Fe4–C42	87.5(2)
Sb1–Fe4–C43	89.4(2)	Sb1–Fe4–C44	176.8(3)
C41–Fe4–C42	118.0(3)	C41–Fe4–C43	121.8(3)
C41–Fe4–C44	89.7(3)	C42–Fe4–C43	119.9(3)
C42–Fe4–C44	95.3(3)	C43–Fe4–C44	90.5(3)
Fe1–C11–O11	173.7(5)	Fe1–C12–O12	163.1(5)
Fe1–C13–O13	176.0(5)	Fe1–C14–O14	176.0(5)
Fe2–C21–O21	174.6(6)	Fe2–C22–O22	163.5(5)
Fe2–C23–O23	177.7(5)	Fe2–C24–O24	175.7(5)
Fe3–C31–O31	177.2(6)	Fe3–C32–O32	175.0(5)
Fe3–C33–O33	179.3(6)	Fe3–C34–O34	178.9(6)
Fe4–C41–O41	176.2(7)	Fe4–C42–O42	176.5(6)
Fe4–43–O43	177.1(5)	Fe4–C44–O44	177.3(8)

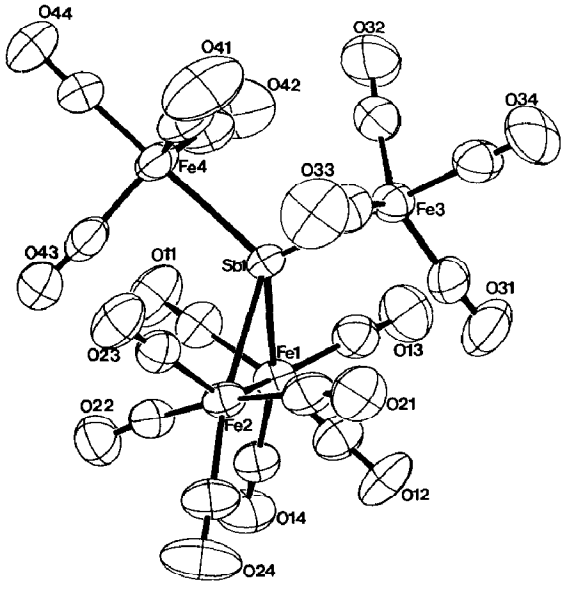

Fig. 1. ORTEP diagram of $[SbFe_4(CO)_{16}]^-$ ($[I]^-$) showing 50% thermal probability ellipsoids and atom labeling. The carbonyl C atoms are left unlabeled for clarity. Their numbering is the same as the oxygen atoms to which they are attached. Bond distances and angles are listed in Table 6.

compared to the lead compound may account in part for the lower degree of bridging character observed for these CO's. The Fe(1)–Fe(2) distance is 2.720(1) Å which falls in the range of the other Fe–Fe single bonds. The Sb atom occupies the axial position on the two trigonal bipyramidal iron atoms of the isolated $Fe(CO)_4$ units. The two iron atoms of the Fe_2 group are in a distorted octahedral coordination sphere.

In Fig. 1. an ORTEP diagram of $[I]^-$ is shown.

Crystal structure of [Et$_4$N]$_2$[II]. The crystal structure of $[Et_4N]_2[II]$ contains ordered $[Sb_2Fe_6(CO)_{20}]^{2-}$ anions and disordered $[Et_4N]^+$ cations in the ratio of 1/2. Selected atomic positional and thermal parameters are given in Table 3 while important bond distances and angles are listed in Table 5. The anion as a distorted octahedral *trans*-Sb_2Fe_4 core in which each Sb atom donates its external lone pair of electrons to an $Fe(CO)_4$ unit. The core geometry is similar to that found for a number of other main group/transition metal cluster compounds including $Co_4(CO)_{11}(GeMe)_2$ [31], $Co_4(CO)_{11}[\mu_4\text{-}GeCo(CO)_4]_2$ [32], (p-tol-P)$_2$Fe$_4$(CO)$_{12}$ [33], (p-tol-P)$_2$Fe$_4$(CO)$_{11}$[P(OMe)$_3$] [34], (p-tol-P)$_2$Fe$_4$(CO)$_{10}$[P(OMe)$_3$] [34], (p-tol-P)$_2$FE$_4$(CO)$_{11}$ [35], $Co_4(CO)_{10}(EPh)_2$ (E = P, As) [36,37], $Fe_2Co_2(CO)_{11}S_2$, [38], $Co_4(CO)_{10}E_2$ (E = S, Se) [39,36a], $(PPh)_2Ru_4(CO)_{11}$ [40], and $Bi_2Ru_4(CO)_{12}$ [41]. The Sb–Fe bond distances within the octahedral core cover a range from 2.517(2) to 2.703(2) Å. The larger values are long compared with the average Sb–Fe bond length 2.666(3) Å found in $[Et_4N]_3[SbFe_4(CO)_{16}]$ [18]. The eight Sb–Fe bonds within the octahedron fall into two sets: the bond distances of Sb(1)–Fe(1) (2.703(2) Å), Sb(1)–Fe(3) (2.640(2) Å), Sb(2)–Fe(2) (2.691(2) Å), and Sb(2)–Fe(4) (2.654(2) Å) are much longer than the other four Sb–Fe bond distances, Sb(1)–Fe(2) (2.517(2) Å), Sb(1)–Fe(4) (2.524(2) Å), Sb(2)–Fe(1) (2.525(2) Å), and Sb(2)–Fe(3) (2.520(2) Å). These distances alternate such that each iron has one long and one

Table 5

Bond distances (Å) and angles (deg) of $[Et_4N]_2[II]\cdot 0.94CH_2Cl_2$

(a) Distances			
Sb1–Fe1	2.702(2)	Sb1–Fe2	2.517(2)
Sb1–Fe3	2.642(2)	Sb1–Fe4	2.521(2)
Sb1–Fe5	2.538(2)	Sb2–Fe1	2.528(2)
Sb2–Fe2	2.692(2)	Sb2–Fe3	2.521(2)
Sb2–Fe4	2.653(2)	Sb2–Fe6	2.538(2)
Fe1–Fe2	2.813(2)	Fe1–Fe4	2.827(2)
Fe2–Fe3	2.824(2)	Fe3–Fe4	2.863(2)
Fe1–C11	1.72(1)	Fe1–C12	1.77(1)
Fe1–C13	1.75(1)	Fe2–C21	1.76(1)
Fe2–C22	1.82(1)	Fe2–C23	1.73(1)
Fe3–C31	1.79(1)	Fe3–C32	1.74(1)
Fe3–C33	1.74(1)	Fe4–C41	1.80(1)
Fe4–C42	1.76(1)	Fe4–C43	1.75(1)
Fe5–C51	1.77(2)	Fe5–C52	1.77(2)
Fe5–C53	1.72(2)	Fe5–C54	1.74(1)
Fe6–C61	1.77(2)	Fe6–C62	1.71(2)
Fe6–C63	1.79(2)	Fe6–C64	1.77(2)
C11–O11	1.16(2)	C12–O12	1.17(2)
C13–O13	1.16(2)	C21–O21	1.13(1)
C22–O22	1.13(2)	C23–O23	1.15(1)
C31–O31	1.13(2)	C32–O32	1.17(1)
C33–O33	1.17(2)	C41–O41	1.14(2)
C42–O42	1.15(1)	C43–O43	1.14(1)
C51–O51	1.12(2)	C52–O52	1.15(2)
C53–O53	1.17(2)	C54–O54	1.17(2)
C61–O61	1.09(2)	C62–O62	1.20(2)
C63–O63	1.14(2)	C64–O64	1.13(2)
(c) Angles			
Fe1–Sb1–Fe2	65.11(5)	Fe1–Sb1–Fe3	96.74(6)
Fe1–Sb1–Fe4	65.44(6)	Fe1–Sb1–Fe5	132.77(6)
Fe2–Sb1–Fe3	66.34(6)	Fe2–Sb1–Fe4	104.66(6)
Fe2–Sb1–Fe5	127.83(7)	Fe3–Sb1–Fe4	67.32(5)
Fe3–Sb1–Fe5	130.49(6)	Fe4–Sb1–Fe5	127.51(6)
Fe1–Sb2–Fe2	65.12(6)	Fe1–Sb2–Fe3	104.59(6)
Fe1–Sb2–Fe4	66.09(5)	Fe1–Sb2–Fe6	130.17(7)
Fe2–Sb2–Fe3	65.52(6)	Fe2–Sb2–Fe4	96.48(6)
Fe2–Sb2–Fe6	133.73(6)	Fe3–Sb2–Fe4	67.15(5)
Fe3–Sb2–Fe6	125.24(8)	Fe4–Sb2–Fe6	129.73(6)
Sb1–Fe1–Sb2	78.68(5)	Fe2–Fe1–Fe4	89.98(7)
Sb1–Fe1–Fe2	54.26(5)	Sb1–Fe1–Fe4	54.19(5)
Sb2–Fe1–Fe2	60.26(5)	Sb2–Fe1–Fe4	59.08(5)
C11–Fe1–Sb1	132.5(5)	C11–Fe1–Sb2	98.3(5)
C11–Fe1–Fe2	157.6(5)	C11–Fe1–Fe4	83.0(4)
C11–Fe1–C12	98.8(6)	C11–Fe1–C13	92.0(6)
C12–Fe1–Sb1	82.8(4)	C12–Fe1–Sb2	160.5(4)
C12–Fe1–Fe2	103.5(4)	C12–Fe1–Fe4	113.9(4)
C12–Fe1–C13	98.4(6)	C13–Fe1–Sb1	135.4(5)
C13–Fe1–Sb2	90.5(5)	C13–Fe1–Fe2	82.6(5)
C13–Fe1–Fe4	147.8(5)	Sb1–Fe2–Sb2	79.06(5)
Sb1–Fe2–Fe1	60.63(5)	Sb1–Fe2–Fe3	58.95(5)
Sb2–Fe2–Fe1	54.62(5)	Sb2–Fe2–Fe3	54.32(5)
Fe1–Fe2–Fe3	90.24(7)	C21–Fe2–Sb1	95.2(5)
C21–Fe2–Sb2	133.8(5)	C21–Fe2–Fe1	154.4(5)

Table 5 (continued)

(c) Angles			
C21–Fe2–Fe3	83.2(5)	C21–Fe2–C22	98.0(6)
C21–Fe2–C23	91.0(7)	C22–Fe2–Sb1	161.5(4)
C22–Fe2–Sb2	82.5(4)	C22–Fe2–Fe1	107.5(4)
C22–Fe2–Fe3	109.9(4)	C22–Fe2–C23	98.1(6)
C23–Fe2–Sb1	94.5(4)	C23–Fe2–Sb2	134.9(4)
C23–Fe2–Fe1	83.2(4)	C23–Fe2–Fe3	152.0(4)
Sb1–Fe3–Sb2	79.95(5)	Sb1–Fe3–Fe2	54.70(5)
Sb1–Fe3–Fe4	54.32(5)	Sb2–Fe3–Fe2	60.16(5)
Sb2–Fe3–Fe4	58.63(5)	Fe2–Fe3–Fe4	89.01(6)
C31–Fe3–Sb1	83.6(4)	C31–Fe3–Sb2	162.9(4)
C31–Fe3–Fe2	106.0(5)	C31–Fe3–Fe4	114.5(5)
C31–Fe3–C32	100.5(7)	C31–Fe3–C33	97.2(6)
C32–Fe3–Sb1	133.6(5)	C32–Fe3–Sb2	87.4(5)
C32–Fe3–Fe2	80.3(5)	C32–Fe3–Fe4	144.9(5)
C32–Fe3–C33	92.8(7)	C33–Fe3–Sb1	132.9(5)
C33–Fe3–Sb2	97.5(5)	C33–Fe3–Fe2	156.7(5)
C33–Fe3–Fe4	84.0(5)	Sb1–Fe4–Sb2	79.75(5)
Sb1–Fe4–Fe1	60.37(5)	Sb1–Fe4–Fe3	58.36(5)
Sb2–Fe4–Fe1	54.83(5)	Sb2–Fe4–Fe3	54.22(5)
Fe1–Fe4–Fe3	89.17(6)	C41–Fe4–Sb1	160.2(4)
C41–Fe4–Sb2	81.8(4)	C41–Fe4–Fe1	102.8(4)
C41–Fe4–Fe3	114.8(5)	C41–Fe4–C42	100.0(6)
C41–Fe4–C43	96.2(7)	C42–Fe4–Sb1	97.5(4)
C42–Fe4–Sb2	131.8(4)	C42–Fe4–Fe1	157.1(4)
C42–Fe4–Fe3	83.1(4)	C42–Fe4–C43	93.7(6)
C43–Fe4–Sb1	91.7(5)	C43–Fe4–Sb2	134.4(4)
C43–Fe4–Fe1	81.9(5)	C43–Fe4–Fe3	148.9(5)
Sb1–Fe5–C51	173.9(5)	Sb1–Fe5–C52	88.4(5)
Sb1–Fe5–C53	90.3(4)	Sb1–Fe5–C54	84.7(4)
C51–Fe5–C52	91.6(7)	C51–Fe5–C53	95.3(6)
C51–Fe1–C54	90.3(6)	C52–Fe5–C53	113.9(7)
C52–Fe5–C54	125.0(8)	C53–Fe5–C54	120.6(8)
Sb2–Fe6–C61	175.0(6)	Sb2–Fe6–C62	86.9(6)
Sb2–Fe6–C63	92.9(5)	Sb2–Fe6–C64	86.0(5)
C61–Fe6–C62	94(1)	C61–Fe6–C63	91.0(8)
C61–Fe6–C64	89.3(8)	C62–Fe6–C63	117.7(9)
C62–Fe6–C64	124.6(8)	C63–Fe6–C64	117.5(9)
Fe1–C11–O11	178(1)	Fe1–C12–O12	174(1)
Fe1–C13–O13	179(1)	Fe2–C21–O21	178(2)
Fe2–C22–O22	169(1)	Fe2–C23–O23	178(1)
Fe3–C31–O31	172(1)	Fe3–C32–O32	176(1)
Fe3–C33–O33	178(1)	Fe4–C41–O41	171(1)
Fe4–C42–O42	177(1)	Fe4–C43–O43	174(1)
Fe5–C51–O51	178(1)	Fe5–C52–O52	177(1)
Fe5–C53–O53	177(1)	Fe5–C54–O54	176(1)
Fe6–C61–O61	176(2)	Fe6–C62–O62	178(2)
Fe6–C63–O63	173(2)	Fe6–C64–O64	176(1)

short Sb–Fe bond. The result is that the Fe_4 square of the octahedron is very puckered. This is also observed in other eight skeletal electron pair clusters listed above. The average Fe–Fe bond distance is long at 2.832(22) Å. The two external Sb–Fe bonds are the same value (2.538(2) Å) and fall in the range of other known

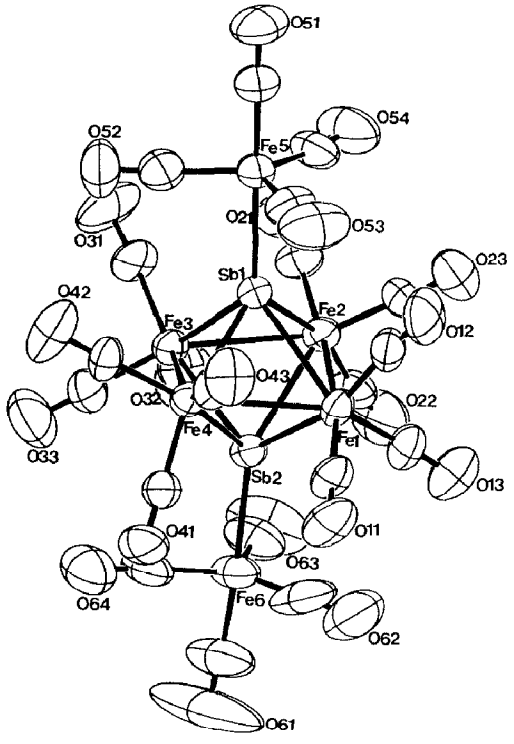

Fig. 2. ORTEP diagram of $[Sb_2Fe_6(CO)_{20}]^{2-}$ ($[II]^{2-}$) showing 50% thermal probability ellipsoids and atom labeling. The carbonyl C atoms are left unlabeled for clarity. Their numbering is the same as the oxygen atoms to which they are attached. Bond distances and angles are listed in Table 7.

Sb–$Fe(CO)_4$ distances (2.460–2.570 Å) [18,28]. Two external iron atoms are trigonal-bipyramidally surrounded by four CO's and an Sb atom which occupies an axial position.

The known examples of E_2M_4 octahedral clusters are seen to possess either seven or eight skeletal electron pairs. $[Et_4N]_2[II]$ falls into the latter category. Seven skeletal pairs are normally expected for an octahedral cluster according to the Wade/Mingos formalism [42]. It has been shown by Hoffmann et al. [43], that the eighth lone pair of electrons in these mixed main group/transition metal octahedral clusters sits in a low lying frontier antibonding b_u orbital of π^* nature which is primarily localized on the four transition metals of the octahedron. As a result of the populating this antibonding π^* orbital, the Fe–Fe bond distances are expected to lengthen as is observed in the anion $[II]^{2-}$.

In Fig. 2 an ORTEP diagram of $[II]^-$ is shown.

Additional material available

Tables of observed and calculated structure factor amplitudes as well as complete listings of atomic positions and bond metricals are available upon request from K.H.W.

Acknowledgement

The National Science Foundation and the Robert A. Welch Foundation are gratefully acknowledged for financial support of this work. The diffractometer with

which the structures reported herein were determined was obtained by the assistance of the National Science Foundation.

References

1 W.A. Herrmann, Angew. Chem. Int. Ed. Engl., 25 (1986) 57.
2 K.H. Whitmire, J. Coord. Chem., 17 (1988) 95.
3 N.C. Norman, Chem. Soc. Rev., 17 (1988) 269.
4 (a) B. Sigwarth, L. Zsolnai, H. Berke and G. Huttner, J. Organomet. Chem., 226 (1982) C5; (b) G. Huttner, U. Weber, B. Sigwarth and O. Scheidsteger, Angew. Chem. Int. Ed. Engl., 21 (1982) 215; (c) G. Huttner, U. Weber and L. Zsolnai, Z. Naturforsch. B, 37 (1982) 707.
5 W.A. Herrmann, B. Koumbouris, A. Schafer, T. Zahn and M.L. Ziegler, Chem. Ber., 118 (1985) 2472.
6 A. Strube, G. Huttner and L. Zsolnai, Angew. Chem. Int. Ed. Eng., 27 (1988) 1529.
7 G. Huttner, U. Weber, B. Sigwarth, O. Scheidsteger, H. Lang and L. Zsolnai, J. Organomet. Chem., 282 (1985) 331.
8 W.A. Herrmann, J. Rohrmann, M.L. Ziegler and T. Zahn, J. Organomet. Chem., 273 (1984) 221.
9 J.M. Cassidy and K.H. Whitmire, Inorg. Chem., 28 (1989) 2494.
10 J.S. Leigh and K.H. Whitmire, Angew. Chem. Int. Ed. Eng., 27 (1988) 396.
11 L.E. Bogan Jr., T.B. Rauchfuss and A.L. Rheingold, Inorg. Chem., 24 (1985) 3722.
12 K. Dehnicke and J. Strahle, Angew. Chem. Int. Ed. Eng., 29 (1981) 413.
13 O.J. Scherer, H. Sitzmann and G. Wolmershäuser, Angew. Chem. Int. Ed. Eng., 24 (1985) 351.
14 K.H. Whitmire, T.A. Albright, S.-K. Kang, M.R. Churchill and J.C. Fettinger, Inorg. Chem., 25 (1986) 2799.
15 K.H. Whitmire, M.R. Churchill and J.C. Fettinger, J. Am. Chem. Soc., 107 (1985) 1056.
16 (a) J.D. Corbett, Prog. Inorg. Chem., 21 (1976) 129; (b) J.D. Corbett, Chem. Rev., 85 (1985) 383; (c) H. Schafer, B. Eisenmann and W. Müller, Angew. Chem. Int. Ed. Eng., 12 (1973) 694; (d) H.G. von Schnering, Angew. Chem. Int. Ed. Eng., 20 (1981) 33.
17 K.H. Whitmire, M. Shieh, C.B. Lagrone, B.H. Robinson, M.R. Churchill, J.C. Fettinger and R.F. See, Inorg. Chem., 26 (1987) 2798.
18 S. Luo and K.H. Whitmire, Inorg. Chem., 28 (1989) 1424.
19 (a) P. Hemmereich and C. Sigwarth, Experientia, 19 (1963) 488; (b) M.G. Simmons, C. Merrill, L.J. Wilson, L.A. Bottomley and K.M. Kadish, J. Chem. Soc. Dalton Trans., (1980) 1827.
20 K.H. Whitmire, J. Ross, C.B. Copper, III., D.F. Shriver, Inorg. Synth., 21 (1982) 66.
21 G.J. Gilmore, MITHRIL: A Computer Program for the Automatic Solution of Crystal Structures from X-Ray Data, University of Glasgow, Scotland, 1983.
22 C.B. Lagrone, K.H. Whitmire, M.R. Churchill and J.C. Fettinger, Inorg. Chem., 25 (1986) 2080.
23 M. Shieh and K.H. Whitmire, Inorg. Chem., 28 (1989) 3164.
24 (a) D. Melzer and E.J. Weiss, J. Organomet. Chem., 255 (1983) 335; (b) A.S. Batsanov, L.V. Rybin, M.I. Rybinskaya, Yu.T. Struchov, I.M. Salimgareeva and N.G. Bogatova, ibid., 249 (1983) 319.
25 P.F. Lindley and P. Woodward, J. Chem. Soc. A, (1967) 382.
26 K.H. Whitmire, C.B. Lagrone, M.R. Churchill, J.C. Fettinger and B.H. Robinson, Inorg. Chem., 26 (1987) 3491.
27 C.F. Campana and L.F. Dahl, J. Organomet. Chem., 27 (1977) 209.
28 K.H. Whitmire, J.S. Leigh, S. Luo, M. Shieh, and M.D. Fabiano, New Journal of Chemistry, 12 (1988) 397.
29 A. Gourdon and Y. Jeanin, J. Organomet. Chem., 304 (1986) C1.
30 F.A. Cotton, G. Wilkinson, Advanced Inorganic Chemistry, 5th Ed., John Wiley & Sons Inc., New York (U.S.A.), 1988, p. 1028.
31 S.P. Foster, K.M. Mackay and B.K. Nicholson, J. Chem. Soc. Chem. Commun., (1982) 1156.
32 S.P. Foster, K.M. Mackay and B.K. Nicholson, Inorg. Chem., 24 (1985) 909.
33 H. Vahrenkamp and D. Wolters, Organometalllics, 1 (1982) 874.
34 T. Jaeger, S. Aime and H. Vahrenkamp, Organometallics, 5 (1986) 245.
35 (a) H. Vahrenkamp, D. Wolters, J. Organomet. Chem., 244 (1982) C17; (b) H. Vahrenkamp and E.J. Wucherer, Chem. Ber., 116 (1983) 1219.
36 (a) R.C. Ryan and L.F. Dahl, J. Am. Chem. Soc., 97 (1975) 6904; (b) R.C. Ryan, C.U. Pittman, J.P. O'Conner and L.F. Dahl, J. Organomet. Chem., 193 (1980) 247.

37 L.D. Lower and L.F. Dahl, J. Am. Chem. Soc., 98 (1976) 5046.
38 H. Vahrenkamp and E.J. Wucherer, Angew. Chem. Int. Ed. Eng., 20 (1981) 680.
39 C.H. Wei and L.F. Dahl, Cryst. Struct. Commun., 4 (1975) 583.
40 J.S. Field, R.J. Haines and D.N. Smit, J. Organomet. Chem. 224 (1982) C49.
41 H.G. Ang, C.M. Hay, B.F.G. Johnson, J. Lewis, P.R. Raithby, and A.J. Whitton, J. Organomet. Chem., 330 (1987) C5.
42 (a) D.M.P. Mingos, Nature Phys. Sci. (London), 236 (1972) 99; (b) K. Wade, Adv. Inorg. Chem., Radiochem., 18 (1976) 1; (c) D.M.P. Mingos, Acc. Chem. Res., 17 (1984) 311.
43 (a) J.-F. Halet, R. Hoffmann and J.-Y. Saillard, Inorg. Chem., 24 (1985) 1695; (b) J.-F. Halet and J.-Y. Saillard, N. J. Chem., 11 (1987) 315.